

NUMERICAL STUDY ON THE EFFECT OF MAGNETIC SHIELD OF A BUNCH SHAPE MONITOR IN J-PARC LINAC

J. Tamura*, H. Ao, A. Miura, N. Ouchi, JAEA/J-PARC, Tokai, Japan
 M. Ikegami, T. Maruta, T. Miyao, K. Takata, KEK/J-PARC, Tokai, Japan

Abstract

In the annual shutdown period of 2012, three bunch shape monitors (BSMs) have been installed to the Japan Proton Accelerator Research Complex (J-PARC) linac beam transport line at the downstream of the separated-type drift tube linac (SDTL). To measure the longitudinal micro-bunch shape of the accelerated H- beam, the BSM detects the electrons produced by the H- beam hitting a wire with negative bias voltage. Due to the space limitation, the each BSM is installed at the center of the quadrupole doublet magnet (QDM), where the fringe field from the quadrupole magnets (QMs) exists. It has been observed that the fringe field significantly affects the orbit of the emitted electrons. To shield the magnetic field, iron plates have been inserted to the spaces between the QMs and BSM. In this paper, numerical estimation of the shield effect is presented.

INTRODUCTION

In 2013, the beam energy of the J-PARC linac is going to be increased from 181 to 400 MeV. This energy upgrade is carried out by adding the Annular-ring Coupled Structure (ACS) linac to the beam transport at the downstream of the SDTL [1]. H- beams are accelerated from 190.8 to 400 MeV using the 21 ACS accelerating modules, two ACS buncher modules (B1, 2), and two ACS debuncher modules (DB1, 2). The J-PARC linac accelerating structures are shown in Fig. 1. These ACS modules are operated at 972 MHz of resonant frequency, while RFQ, DTL and SDTL are operated at 324 MHz. The longitudinal matching of the beam injected into the ACS is one of the key issues for the energy upgrade.

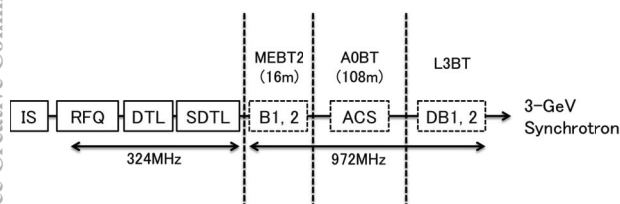


Figure 1: Diagram of J-PARC linac accelerating structures.

To measure the longitudinal micro-bunch shape of the accelerated H- beam, three BSMs have been installed in the beginning part of the ACS in the annual shutdown period of 2012 [2, 3]. Due to the space limitation, each BSM is installed at the center of the QDM (Fig. 2). In the energy

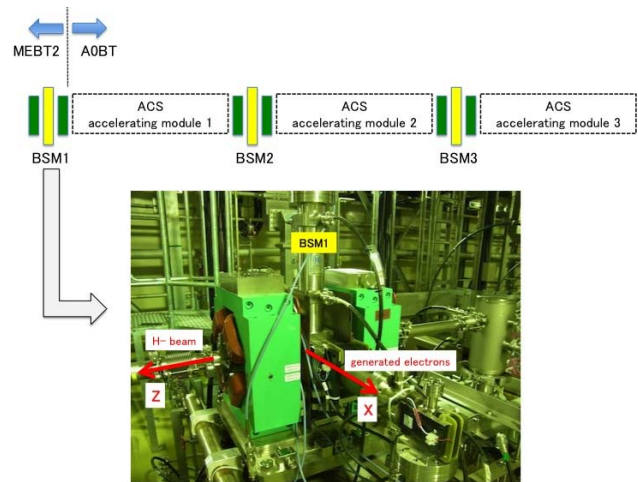


Figure 2: Installation location of the BSMs.

upgrade period of 2013, the first, second and third accelerating module of ACS will be installed after the BSM1, BSM2 and BSM3, respectively. In the present 181 MeV beam operation, the 16th SDTL tank A is used for the first debuncher module in the ACS3 section, while the other debuncher module (16th SDTL tank B) is in L3BT.

FRINGE FIELD EFFECT OF QDM

In the BSM, the electrons produced by the H- beam hitting a wire with negative bias voltage are detected [4]. As shown in Fig. 3, the produced electrons are focused by the electrostatic lens effect of parallel plate electrode between

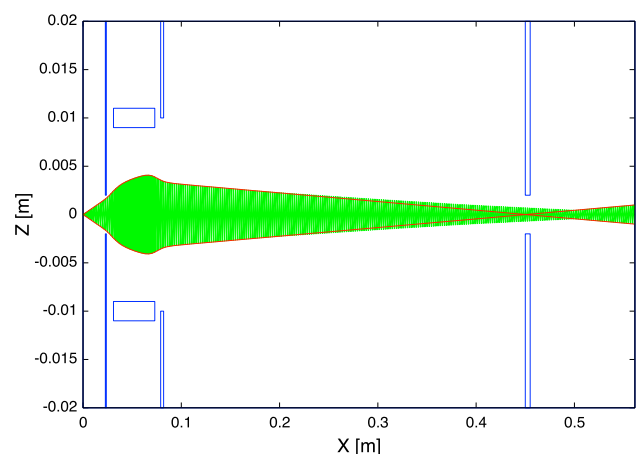


Figure 3: Electron orbit in the BSM.

*jtamura@post.j-parc.jp

the first and second slits, and detected by the electron multiplier about 55 cm far from the wire. In the practical operation of the BSM to measure the micro-bunch shape of the H- beam, the phase of the RF to deflect the electrons to z direction is shifted and only the electrons passing through the third slit are detected.

In J-PARC, the each BSM is installed at the center of the QDM where the fringe field of the QMs exists. This make the BSM measurement difficult because the electron orbit is significantly affected by this field. To investigate the effect of the fringe field on the electron orbit in the BSM, the magnetic field generated by the QDM has been simulated using CST EM STUDIO. The magnetic pole length and the gap length of each QM of the QDM where BSM1 is installed is 120 mm and 180 mm, respectively. This QDM is excited by the coils of 27 turns per pole with the rated current of 250 A. The magnetic pole length and the gap length of each QM of the QDMs where BSM2 and BSM3 are installed is 135 mm and 180 mm, respectively. This QDM is excited by the coils of 32 turns per pole with the rated current of 200 A. In the energy upgrade of the J-PARC linac, these 135 mm QDMs are replaced by the 120 mm QDMs. In this paper, we focus on the magnetic field generated by the 120 mm QDM (Fig. 4).

The magnetic field B_y along x direction (horizontal) at the center of the magnetic pole ($z = \pm 150\text{mm}$) is shown in Fig. 5. The field B_y is linear with x within 45 mm of bore aperture of the QM. The magnetic field near the center of the QDM ($z = \pm 10\text{mm}$ and $z = \pm 20\text{mm}$) is shown in Fig. 6. The BSM detects the electrons advancing toward

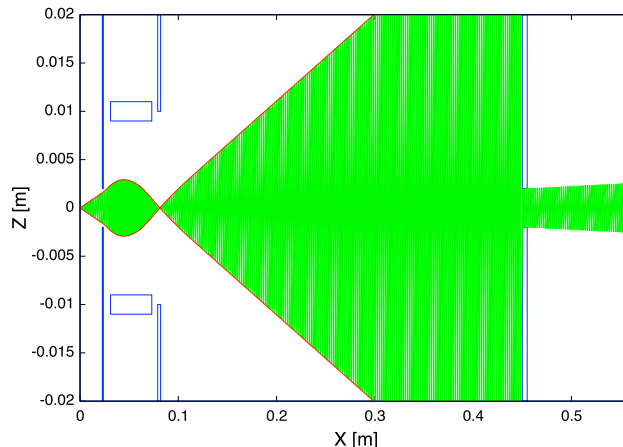


Figure 7: Electron orbit bent by the fringe field of the QDM.

$+x$ direction. This magnetic field rotate the electrons inward because these electrons are bended by B_y at $z < 0$ to $+z$ direction and by B_y at $z > 0$ to $-z$ direction. This make the electron beam over-focusing and prevent most of them from reaching the detector (Fig. 7).

MAGNETIC SHIELDING

To shield the magnetic field, iron plates have been inserted to the spaces between the QMs and BSM (Fig. 8). The dimension of the outer two plates is 350mm (Δx) 350mm (Δy) 1mm (Δz) with 90 mm of bore aperture in

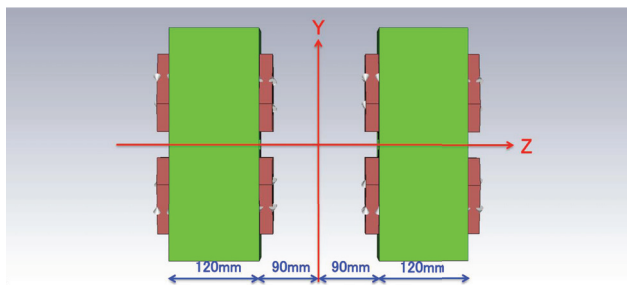


Figure 4: Simulation model of the QDM.

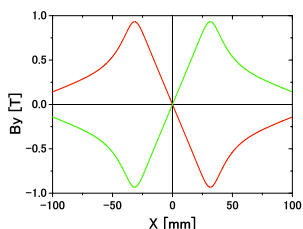


Figure 5: Magnetic field at the center of the magnetic pole (red line: $z = -150\text{mm}$, green line: $z = +150\text{mm}$).

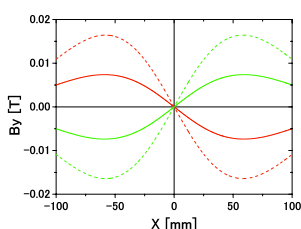


Figure 6: Magnetic field near the center of the QDM (red line: $z = -10\text{mm}$, green line: $z = +10\text{mm}$, dashed red line: $z = -20\text{mm}$, dashed green line: $z = +20\text{mm}$).

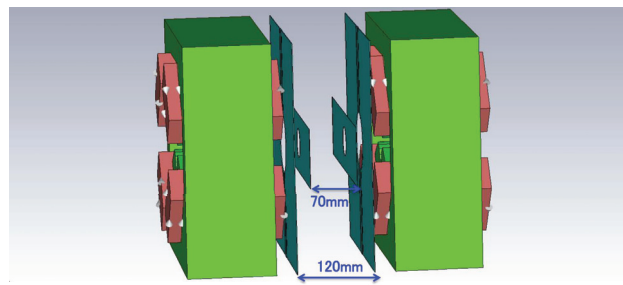


Figure 8: Simulation model of the QDM with shield.

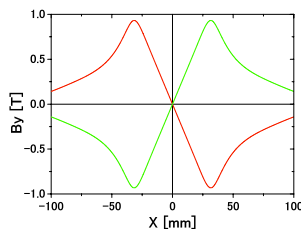


Figure 9: Magnetic field with shield at the center of the magnetic pole (red line: $z = -150\text{mm}$, green line: $z = +150\text{mm}$).

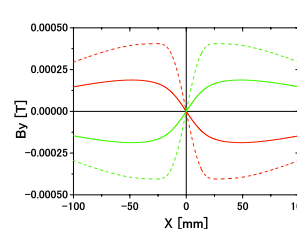


Figure 10: Magnetic field with shield near the center of the QDM (red line: $z = -10\text{mm}$, green line: $z = +10\text{mm}$, dashed red line: $z = -20\text{mm}$, dashed green line: $z = +20\text{mm}$).

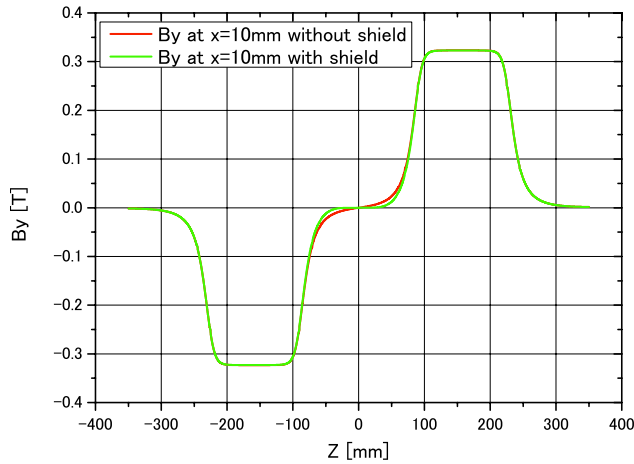


Figure 11: Magnetic field with and without shield at $x = +10\text{mm}$.

its center. The thickness (Δz) of these plates in the center region of 20mm (Δx) 350mm (Δy) is 2 mm due to the overlap of the two plates. The dimension of the inner two plates is 350mm (Δx) 90mm (Δy) 0.4mm (Δz) with 45 mm of bore aperture in its center. In the numerical simulation, the magnetic permeability of the iron plates is set to $1000\mu_0$ where μ_0 is permeability of vacuum. The simulation result for the magnetic field at the center of the magnetic pole and near the center of the QDM are shown in Fig. 9 and Fig. 10, respectively. Comparing these figures with Fig. 5 and Fig. 6, the magnetic field only near the center of the QDM become 40 times smaller with the shield. The reduction of the magnetic field in the center region of the QDM enables us to utilize the BSM.

These magnetic shield cause the difference of the integrated magnetic field gradient (GL). The magnetic field B_y at $x = +10\text{mm}$ is shown in Fig. 11. One can see that magnetic field with shield is smaller than that without shield inside the two QMs. GL, which is obtained by integrating $\Delta B_y / \Delta x$ by z , is decreased to 98.7% by installing the shield.

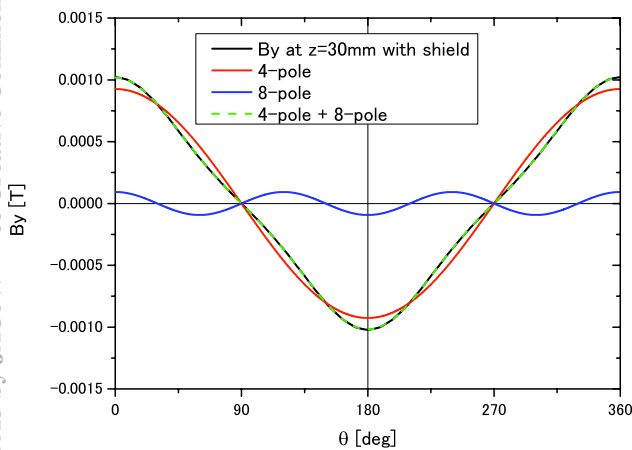


Figure 12: Superposition of the multi-pole component of the magnetic field with shield at $z = +30\text{mm}$.

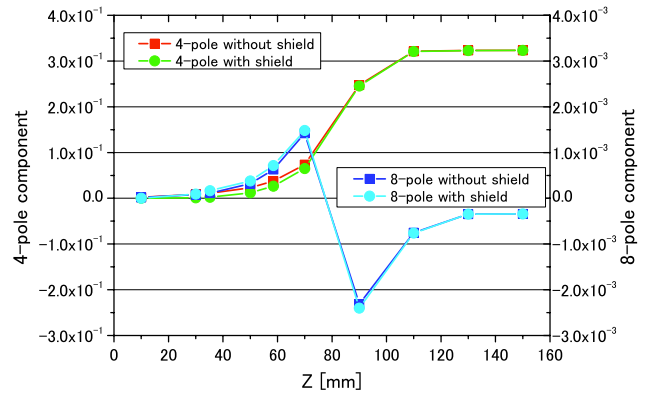


Figure 13: Multi-pole component of the magnetic field with and without shield.

To estimate the multi-pole component of the field, B_y at $r = 10\text{mm}$ ($0 < \theta < 360$) is expanded by cosine. The coefficient of $\cos \theta$, $\cos 2\theta$, $\cos 3\theta$, $\cos 4\theta$, ... shows the strength of 4-pole, 6-pole, 8-pole, 10-pole, ..., respectively. As an example, superposition of the multi-pole component of the field with shield at $z = +30\text{mm}$ is shown in Fig. 12. As a higher pole component, only the 8-pole component appears over z . The field strength of 4-pole and 8-pole is shown in Fig. 13. The strength of 8-pole is smaller than 4-pole in two order. The 8-pole component is considered to be unrealistic because it has no change between with and without the shield. In spite of the asymmetry of the shield shape, higher-order component doesn't appear.

SUMMARY

In J-PARC linac, BSMs have been installed to the center of the QDMs in the the beam transport line. To shield the fringe field of the magnet, iron plates have been inserted between the BSM and QMs. Numerical simulation shows that the integrated magnetic field gradient (GL) is decreased to 98.7% and multi-pole component is negligibly small. We found that there aren't any problem with the magnetic field shielding for beam operation.

ACKNOWLEDGEMENT

We gratefully acknowledge indispensable contribution of A.V. Feschenko and his colleagues in INR on magnetic field simulation.

REFERENCES

- [1] H. Ao et al., "Annular-ring coupled structure linac for the J-PARC linac energy upgrade", in these proceedings.
- [2] A. Miura et al., "Bunch shape measurement of 181 MeV beam in J-PARC linac", in these proceedings.
- [3] M. Ikegami et al., "Recent progress in beam commissioning of J-PARC linac", in these proceedings.
- [4] A.V. Feschenko, "Methods and instrumentation for bunch shape measurements," PAC'01, Chicago, June 2001, p. 517.